Neuron, Vol. 48, 31–43, October 6, 2005, Copyright ©2005 by Elsevier Inc. DOI 10.1016/j.neuron.2005.08.024

Math1 Expression Redefines the Rhombic Lip Derivatives and Reveals Novel Lineages within the Brainstem and Cerebellum

Vincent Y. Wang,[1,3] Matthew F. Rose,[1,3] and Huda Y. Zoghbi[1,2,*]
[1]Program in Developmental Biology
[2]Howard Hughes Medical Institute
Departments of Pediatrics
Molecular and Human Genetics
Baylor College of Medicine
One Baylor Plaza
Houston, Texas 77030

Summary

The rhombic lip (RL) is an embryonic proliferative neuroepithelium that generates several groups of hindbrain neurons. However, the precise boundaries and derivatives of the RL have never been genetically identified. We use β-galactosidase expressed from the *Math1* locus in *Math1*-heterozygous and *Math1*-null mice to track RL-derived cells and to evaluate their developmental requirements for *Math1*. We uncover a *Math1*-dependent rostral rhombic-lip migratory stream (RLS) that generates some neurons of the parabrachial, lateral lemniscal, and deep cerebellar nuclei, in addition to cerebellar granule neurons. A more caudal *Math1*-dependent cochlear extramural stream (CES) generates the ventral cochlear nucleus and cochlear granule neurons. Similarly, mossy-fiber precerebellar nuclei require *Math1*, whereas the inferior olive and locus coeruleus do not. We propose that *Math1* expression delimits the extent of the rhombic lip and is required for the generation of the hindbrain superficial migratory streams, all of which contribute neurons to the proprioceptive/vestibular/auditory sensory network.

Introduction

Over a century ago, His identified the region along the dorsal edge of the fourth ventricle of two-month-old human embryos as the "Rautenlippe" (rhombic lip, RL) (His, 1891). Present in all vertebrates, the RL is the dorsal-most portion of the hindbrain proliferative neuroepithelium (Wingate, 2001). It can be divided along the long axis of the hindbrain into rostral (rRL) and caudal (cRL) portions that assume dorsal and ventral positions, respectively, as the brainstem bends during development (Altman and Bayer, 1997).

The rRL is classically thought to generate only cerebellar granule neurons (Altman and Bayer, 1997). Granule neuron progenitors migrate superficially from the rRL starting at mouse embryonic day 13 (E13) to form the external granule layer (EGL) on the surface of the cerebellum. These cells proliferate to form the granule neurons, which subsequently descend into the cerebellum (Hatten and Heintz, 1995). Other cerebellar cell types such as inhibitory Purkinje cells (PCs) and efferent deep nuclear neurons (DNs) begin forming around E10 (Taber-Pierce, 1975) and are thought to derive from a more ventromedial portion of the ventricular neuroepithelium, classically called the "ventricular zone" (Hallonet et al., 1990; Hatten and Heintz, 1995; Hoshino et al., 2005; Mathis et al., 1997). Curiously, radioactive thymidine labeling suggests that DNs first aggregate in a superficial "Nuclear Transitory Zone" (NTZ), similar in position to the later-forming EGL, before descending into the deep cerebellum (Altman and Bayer, 1985).

In contrast, the cRL is thought to generate the entire cochlear nucleus (CN) (Altman and Bayer, 1980; Harkmark, 1954; Ivanova and Yuasa, 1998). The CN is divided anatomically into dorsal (DC) and ventral (VC) subunits containing many different cell types, including cochlear granule neurons, inhibitory cartwheel cells, and deep efferent neurons (Taber-Pierce, 1967). These cell types and the organization of the CN is similar to that of the cerebellum (Oertel and Young, 2004).

A more caudal portion of the cRL is thought to generate the five main brainstem "precerebellar" nuclei that relay peripheral sensation and cortical input to the cerebellum. Four of these nuclei project mossy fibers to the cerebellar granule neurons and DNs and are thought to migrate in superficial "extramural" streams, reminiscent of the EGL (Altman and Bayer, 1987c, 1987d). In contrast, the inferior olive precerebellar nucleus (ION) projects climbing fibers to the PCs and is thought to form via an intramural migratory stream (Altman and Bayer, 1987b). Several recent studies suggest that mossy-fiber neurons may be more developmentally related to cerebellar granule neurons than to ION neurons (Funfschilling and Reichardt, 2002; Li et al., 2004; Rodriguez and Dymecki, 2000).

Since His' initial analysis, many attempts have been made to further define the RL and to identify the cells that derive from it. Yet, the distinction between the RL and the adjacent ventricular neuroepithelium remains loosely defined by an anatomical bend that forms late in development (Altman and Bayer, 1987a). Hence, a precise definition of the RL and a clear demonstration of its derivatives are lacking.

The basic helix-loop-helix transcription factor *Mouse atonal homolog 1* (*Math1*, *Atoh1*) is expressed in the RL as early as E9.5 (Akazawa et al., 1995). *Math1* is required for the development of the cerebellar granule neurons and at least two of the mossy-fiber nuclei, but not for the ION (Ben-Arie et al., 1997, 2000; Bermingham et al., 2001). Interestingly, these known *Math1*-dependent RL derivatives do not begin to form until E13, when the RL becomes anatomically distinguishable, even though *Math1* expression begins much earlier. Developmental studies show that molecular markers often identify regional domains more precisely than do anatomical landmarks because gene expression often precedes the anatomical changes (Millet et al., 1996; Wingate and Hatten, 1999). Thus, this earlier *Math1* expression may identify the extent of the early RL and

*Correspondence: hzoghbi@bcm.edu
[3]These authors contributed equally to this work.

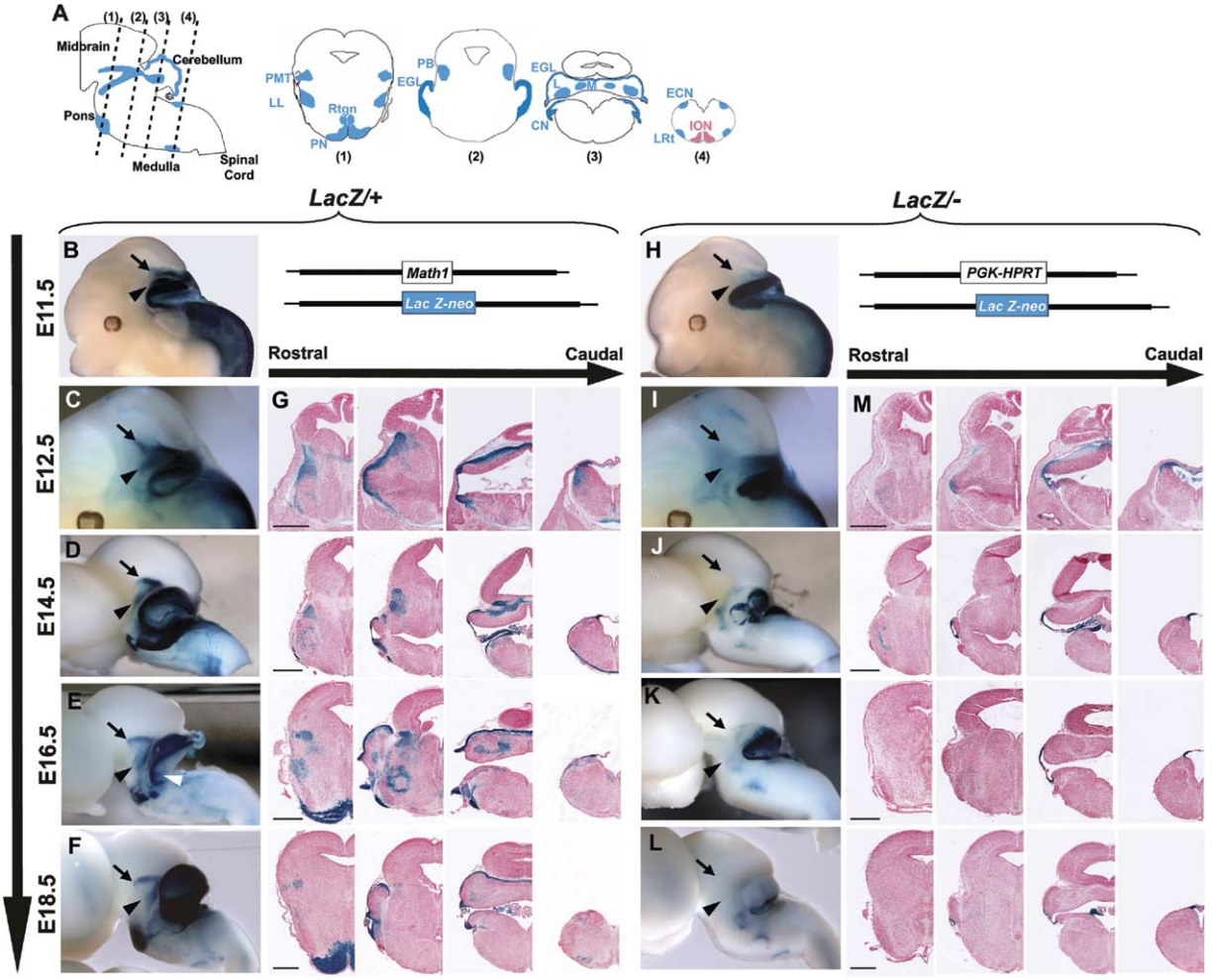

Figure 1. β-Galactosidase Expression in *Math1*-Heterozygous and -Null Embryos

All whole mounts are oriented with rostral to the left. All coronal hemisections are oriented with lateral to the left. (A) Schematics of β-gal expression in an E18.5 *Math1*$^{LacZ/+}$ embryo: parasagittal (left) and coronal sections from levels indicated by dotted lines 1, 2, 3, and 4. (B–G) β-gal expression in *LacZ*/+ whole-mount embryos (B and C) or brains (D–F) from E11.5–E18.5 and in corresponding coronal sections (G). Schematic shows the two alleles of the heterozygote: one wild-type (+) and one LacZ knockin null allele (*LacZ*). β-gal+ cells of the RLS are indicated in the isthmus/PMT (black arrows) and along the LL in the pons (black arrowheads). The AES is partially removed in (E) to better visualize β-gal expression in the CN (white arrowhead). (H–M) β-gal expression in *Math1*$^{LacZ/-}$ littermates is greatly reduced and mostly localized to the RL. The *LacZ*/– embryos have the same copy number of the *LacZ* gene as *LacZ*/+ embryos because they have an *HPRT* null allele (–) rather than a second *LacZ* allele. Arrows and arrowheads indicate missing RLS β-gal expression in the isthmus and pons. Abbreviations: CN, cochlear nucleus; ECN, external cuneate nucleus; EGL, external granule layer; ION, inferior olive nucleus; L, lateral deep cerebellar nucleus; LL, lateral lemniscus; LRt, lateral reticular nucleus; M, medial deep cerebellar nucleus; PB, parabrachial nucleus; PMT, pontomesencephalic tegmentum; PN, pontine nucleus; Rtgn; reticulotegmental nucleus. Scale bars, 500 μm (G and M).

indicate a role of *Math1* in previously unrecognized rhombic-lip derivatives.

To better define the rhombic lip and the neurons it generates, we use a *LacZ* reporter gene targeted to the *Math1* locus (Ben-Arie et al., 2000). The transient *LacZ* mRNA expression within the RL tags the cells with β-galactosidase protein (β-gal) and allows their migration to be tracked for several days while the β-gal persists. This approach has worked well to trace other cell lineages in the central nervous system (Bermingham et al., 2001; Zhou and Anderson, 2002). We demonstrate that *Math1* identifies and is necessary for the development of both known and novel superficial migratory neurons of the hindbrain. These neurons include most cells thought to derive from the RL as well as novel RL derivatives. Based on these observations, we propose a genetic definition of the rhombic lip as the *Math1*-expressing region of the hindbrain ventricular neuroepithelium and identify several novel rhombic-lip derivatives in the isthmus, pons, and cerebellum.

Results

β-Galactosidase Labels Cells Derived from *Math1*-Expressing Progenitors in the Rhombic Lip

We follow β-gal expression from E11.5 to E18.5 in both *Math1*-heterozygous (*Math1*$^{LacZ/+}$) and *Math1*-null (*Math1*$^{LacZ/-}$) embryos (Figures 1A–1M). To ensure

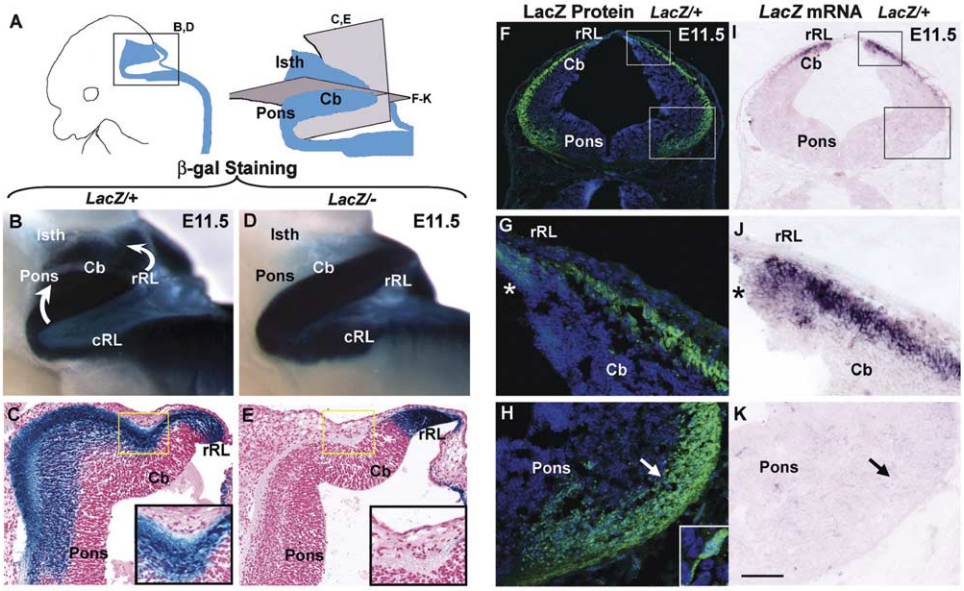

Figure 2. The Rostral Rhombic-Lip Migratory Stream (RLS)

(A) Two schematics are shown. A drawing depicting an E11.5 whole-mount embryo (left) indicates the region of close up shown at right and in (B) and (D). Parasagittal and horizontal planes through the close-up schematic indicate the levels of section shown in (C) and (E) and (F)–(K), respectively.

(B–E) Whole mounts at E11.5 show β-gal expression along the entire length of the RL of both *Math1*$^{LacZ/+}$ (B) and *Math1*$^{LacZ/-}$ (D) embryos. Curved arrows (B) indicate proposed RLS from the rRL to the isthmus, pons, and cerebellum. Corresponding parasagittal sections show the stream of β-gal+ cells and their β-gal+ fiber tracts in the *LacZ*/+ embryo (C) and the absence of the RLS in the *LacZ*/– embryo (E). Insets show regions bounded by yellow boxes. Dorsal is to the right.

(F–K) Adjacent horizontal sections show differential localization of LacZ protein (green) (F–H) and mRNA transcript (purple) (I–K) in E11.5 *LacZ*/+ embryos. Boxes in (F) and (I) are shown at high power in (G) and (H) and (J) and (K), respectively. Both *LacZ* mRNA and LacZ protein are present in the rRL (G and J), but only LacZ protein is present in the pons (H and K). RLS cells in pons (arrow) have characteristic migratory unipolar morphology (H, inset). Asterisks in (G and J) indicate ventricular surface of rRL. Dorsal is up. Abbreviations: Cb, cerebellum; cRL, caudal rhombic lip; Isth, isthmus; rRL, rostral rhombic lip. Scale bar, 160 μm (C and E); 250 μm (F and I); 45 μm (G and J); 65 μm (H and K).

equal dosing of the *LacZ* gene, both genotypes carry only one copy of the *Math1*^{LacZ} null allele. Coronal sections through the *Math1*$^{LacZ/+}$ hindbrain show β-gal+ cells in the isthmus, pons, cerebellum, and medulla (Figure 1G). For each of these regions, a stream of β-gal+ cells can be traced back to the rhombic lip (RL). In contrast, the β-gal expression in *Math1*$^{LacZ/-}$ embryos is primarily in the RL (Figure 1M). Sagittal and horizontal sections at each time point verify the three-dimensional localization of the β-gal+ cells, and β-gal antibody labeling demonstrates that this staining is not due to background galactosidase activity (Figures 2B–2H and data not shown).

The Rostral Rhombic-Lip Migratory Stream Requires *Math1* and Gives Rise to Cells in the Isthmus, Pons, and Cerebellum

β-galactosidase staining is present in the isthmus, pons, and cerebellum of *Math1*$^{LacZ/+}$ embryos at E11.5, several days before the migration of known RL-derived neurons (Figures 2B and 2C). However, along the ventricular neuroepithelium, β-gal is present only at the RL and is absent from the remainder of the cerebellar, pontine, and isthmic ventricular neuroepithelia (Figure 2C). There are two potential explanations for these observations. The β-gal-expressing cells in the pons represent either unidentified migratory derivatives of the RL or ectopic expression of the *Math1*^{LacZ} allele within the pons itself. To distinguish these possibilities, we analyzed adjacent serial horizontal sections for *LacZ* mRNA and protein expression. *LacZ* mRNA is present in the developing rostral RL (rRL) (Figures 2I and 2J) but not in the pons (Figure 2K), matching the known *Math1*-mRNA expression pattern (Akazawa et al., 1995). In contrast, LacZ protein is present in both the rRL and the pons (Figures 2F–2H), and many of the cells containing LacZ protein have a unipolar morphology (Figure 2H, inset) characteristic of migrating RL-derived cells (Wingate and Hatten, 1999). These results indicate that the β-gal staining in the pons is most likely due to the persistence of the LacZ protein in cells derived from the RL rather than ectopic *LacZ* mRNA expression. Because the known pontine RL derivatives do not reach the pons until after E13 (Marillat et al., 2004; Taber-Pierce, 1966), these early β-gal+ cells represent novel derivatives of the rRL. We term this migration the "rostral rhombic-lip migratory stream" (RLS). In the absence of *Math1*, the RLS does not form (Figures 2D and 2E).

To better characterize the RLS cell population, we next examined the hindbrain after RLS migration was complete. At E16.5, cells in the rostral-most portion of the RLS are located in two general regions (Figures 3A–

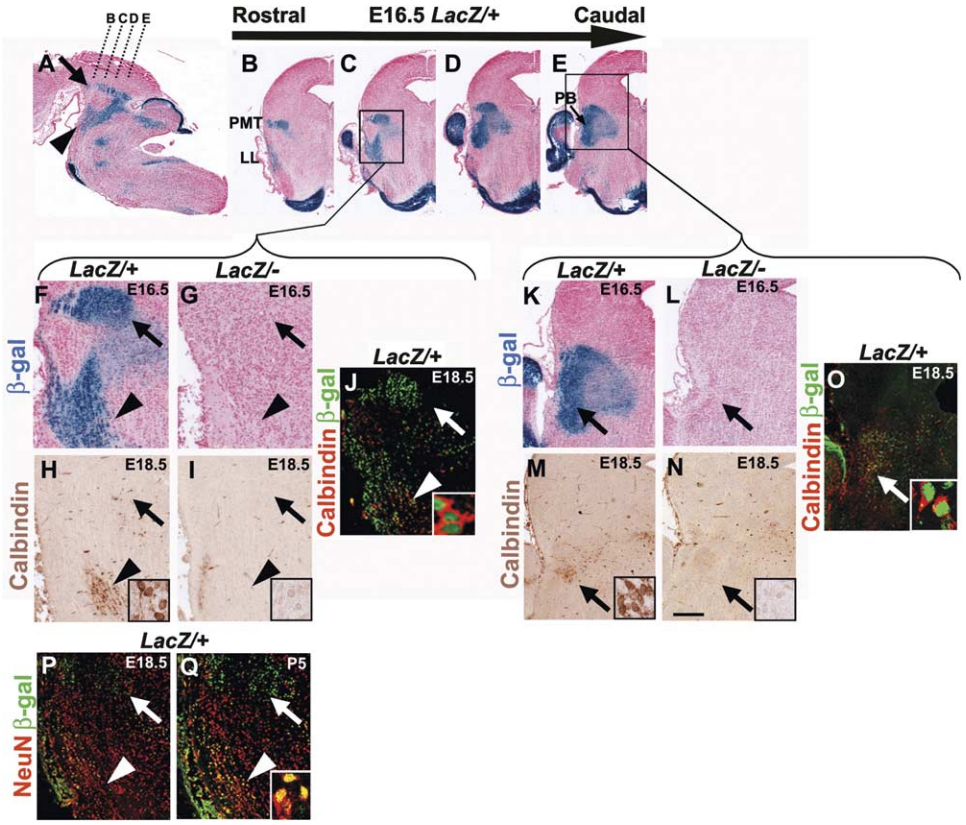

Figure 3. Rostral Rhombic-Lip-Derived Neurons of the Isthmus and Pons Require *Math1*

All coronal sections are oriented with lateral to the left. (A–E) Parasagittal section of an E16.5 *Math1*$^{LacZ/+}$ embryo (A) shows β-gal+ cells of the RLS in the isthmus/PMT (arrow) and along the LL in the pons (arrowhead) (rostral oriented to the left). Dotted lines show the levels of serial coronal sections shown in (B–E). Boxes indicate regions of close up shown in corresponding bracketed panels. (F–J) Perilemniscal cells (arrowheads) express β-gal (F) and calbindin (H), both of which are lost in *Math1*$^{LacZ/-}$ embryos (G and I). LacZ protein and calbindin colocalize in the same cells (J, inset). β-gal expression is also lost from the PMT (arrows) in *LacZ/–* embryos (G). (K–O) Lateral parabrachial cells also express β-gal (K) and calbindin (M), both of which are similarly lost in *LacZ/–* embryos (L and N). LacZ protein and calbindin again colocalize in some cells (O, inset). (P and Q) β-gal+ perilemniscal cells (arrowheads) express NeuN at E18.5 (P) and at P5 (Q, inset). Some β-gal+ PMT cells (arrow) begin to express NeuN at P5 (Q). Abbreviations: LL, lateral lemniscus; P5, postnatal day five; PB, parabrachial nucleus; PMT, pontomesencephalic tegmentum. Scale bar, 400 μm (A–E); 100 μm (F–J and P–Q); 180 μm (K–O).

3E). One group of β-gal+ cells settles in the pons along the developing nuclei of the lateral lemniscus (LL) (Figures 3A and 3F, arrowheads). These nuclei include dorsal (DLL), intermediate (ILL), and ventral (VLL) divisions, along with a perilemniscal zone, and are important components of the auditory system (Friauf, 1994). A second group of β-gal+ cells settles at the junction of the pons and midbrain, the pontomesencephalic tegmentum (PMT, isthmus) (Figures 3A, 3F, and 3K, arrows). The caudal portion of the PMT includes the parabrachial nuclei (PB) which surround the output tract of the cerebellum (Paxinos et al., 1994) and appear to integrate proprioceptive and vestibular input with autonomic functions (Balaban et al., 2002). Previous studies show that the majority of calbindin-expressing cells of the LL are localized to the perilemniscal zone at E18.5 (Friauf, 1994; Jacobowitz and Abbott, 1997). In the PMT, the lateral parabrachial nucleus also expresses calbindin at this time (Jacobowitz and Abbott, 1997; Paxinos et al., 1999). We find cells expressing calbindin in both the LL (Figure 3H, arrowhead, inset) and PMT (Figure 3M, arrow, inset), and some of them colocalize with β-gal-expressing cells in both regions (Figures 3J and 3O, insets). In the absence of *Math1*, the LL and PMT lose both the β-gal (Figures 3G and 3L) and calbindin staining (Figures 3I and 3N). Additional staining with NeuN shows that β-gal+ cells in the LL differentiate into neurons (Figures 3P and 3Q, arrowheads). The development of these cells could not be followed further because their β-gal levels become undetectable. Overall, these results identify novel derivatives of the rhombic lip in the lateral lemniscus and pontomesencephalic tegmentum of the hindbrain.

Deep Cerebellar Neurons and the External Granule Layer Arise Sequentially from the Rostral Rhombic Lip and Are *Math1* Dependent

At E11.5, the caudal portion of the RLS covers the entire dorsal surface of the developing cerebellum (Figure 4A), and from E12.5 to E14.5, these β-gal+ cells aggregate in the rostral cerebellum (Figures 4B–4D and 4V). This position correlates with the nuclear transitory zone

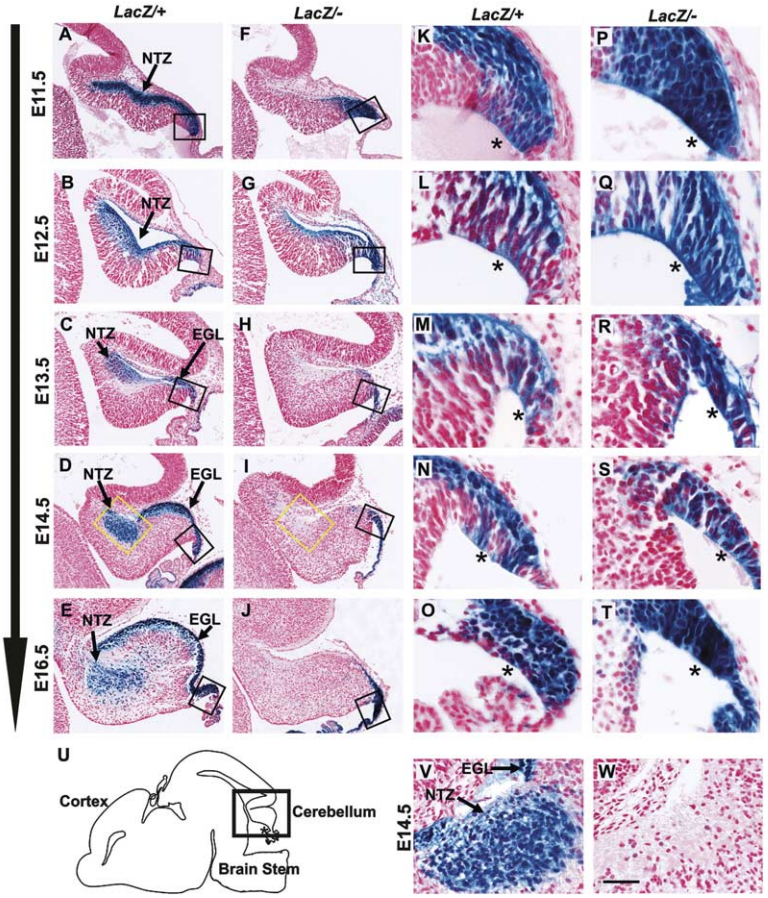

Figure 4. The Nuclear Transitory Zone and External Granule Layer Arise Sequentially from the Rostral Rhombic Lip and Require *Math1*

All sagittal sections are oriented with rostral to the left. (A–J) Parasagittal sections through *Math1*$^{LacZ/+}$ embryos from E11.5 to E16.5 show β-gal+ cells of the RLS covering the dorsal surface of the cerebellum first in the position of the NTZ and then in the position of the EGL (A–E). The NTZ β-gal+ cells appear to aggregate rostrally as the EGL forms (D) and then descend into the deep cerebellum (E). The NTZ and EGL are absent in *Math1*$^{LacZ/-}$ embryos (F–J), and only a few β-gal+ fibers appear on the cerebellar surface at E12.5 (G). (K–T) The rRL bends and changes shape from E11.5 to E16.5 but maintains β-gal expression throughout this time in both *LacZ*/+ (K–O) and *LacZ*/– (P–T) embryos. (Boxed regions in [A]–[E] are rotated to maintain the same orientation of the rRL ventricular surface, indicated by asterisks.) (U) Schematic of parasagittal section from an E18.5 mouse brain. Box shows region of close-up in (A–J). (V and W) Close ups of the yellow-boxed regions in (D) and (I) show that the NTZ is replaced by a relatively acellular, fibrous region in the *LacZ*/– embryos. Abbreviations: EGL, external granule layer; NTZ, nuclear transitory zone. Scale bar, 180 μm (A–J); 30 μm (K–T); 50 μm (V and W).

(NTZ), a proposed transient differentiation zone for cells destined to become deep nuclear neurons (DNs) of the cerebellum (Altman and Bayer, 1985). This region also corresponds to the developing superior cerebellar peduncle (SCP), the primary output fiber tract of DNs (Altman and Bayer, 1997). β-gal+ fibers are present in both the SCP and uncinate fasciculus (hook bundle of Russell), another fiber tract of the DNs (data not shown). From E14.5 to E16.5, this β-gal+ aggregation descends into the deep cerebellum, as is theorized for the NTZ (Figure 4E). During this same time, the most caudal portion of the RLS remains superficial and forms the EGL (Figures 4C–4E). Although the precise boundary between the NTZ and EGL is not clear at E13.5, the general regions of these two populations can be discerned. Higher magnification views at E11.5 to E16.5 show a continuous stream of β-gal+ cells exiting the rRL (Figures 4K–4O). During this time, the rRL bends to form the classical "germinal trigone" shape (Figure 4N) that has been used to define the extent of the rRL (Altman and Bayer, 1985). Importantly, in the absence of *Math1*, the NTZ and EGL are both lost (Figures 4F–4J and 4W), although cells in the rRL continue to express β-gal (Figures 4P–4T).

We next used morphology and known molecular markers to assess whether loss of the NTZ in *Math1*$^{LacZ/-}$ embryos correlates with loss of deep nuclear neurons of the cerebellum. Coronal sections at E16.5 show that NTZ cells settle in one medial and one lateral aggregate within each cerebellar hemisphere (Figure 5B). These positions correspond with previously described positions of the nucleus medialis (fastigial) and nucleus lateralis/intermedius (dentate/interpositus) of the developing deep cerebellar nuclei (Altman and Bayer, 1997). Hence, the β-gal+ cells followed in Figure 4 settle in the region of the fastigial nucleus (Figure 5D). This position corresponds at E18.5 with a cluster of large cells (Figure 5F) that express *LIM-homeodomain nine* (*Lhx9, Lh2b*) (Figure 5H) and *T-box related one* (*Tbr-1*) (Figure 5J) transcription factors. High magnification views show that Tbr-1 is localized to cells with large nuclei, as demonstrated by TOTO-3 nuclear colabeling (Figures 5L–5O, arrows). *Lhx9* is known to be expressed by other *Math1*-dependent cells (Bermingham et al., 2001), and *Tbr-1* is known to label DNs of the developing fastigial nucleus (R. Hevner, personal communication). *Lhx9* also labels the region of the dentate/interpositus nucleus (data not shown). In the absence of *Math1*, Nissl staining shows gross disruption of the cytoarchitecture of the deep cerebellum (Figure 5G). The expected region of the fastigial nucleus lacks β-gal, *Lhx9*, and Tbr-1 staining (Figures 5E, 5I, and 5K) and shows a loss of cells with large nuclei (Figures 5P–5S). Similarly, the expected region of the dentate/interpositus nucleus shows a loss of β-gal and *Lhx9* staining (data not shown). Instead, these regions contain ec-

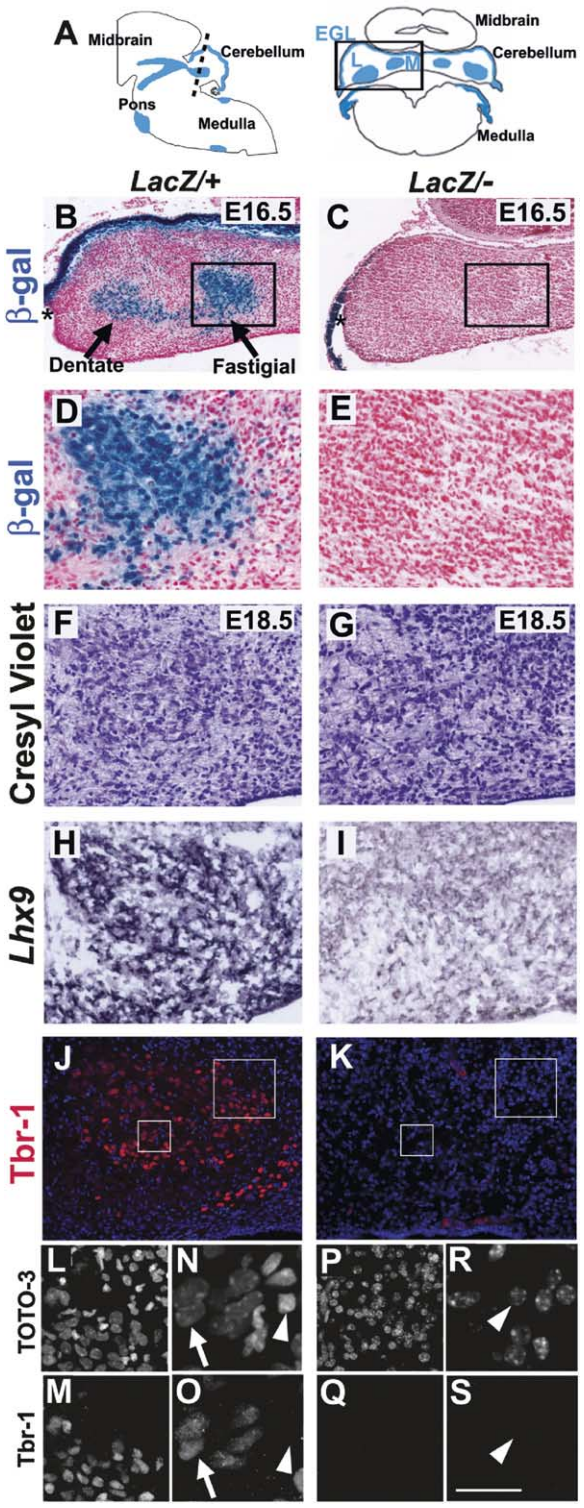

Figure 5. Deep Cerebellar Neurons Arise from the Rostral Rhombic Lip and Require *Math1*

All coronal sections are oriented with lateral to the left. (A) Two schematics are shown. A parasagittal section through the hindbrain (left), with a dotted line indicating the level of coronal section at right. The box in the coronal section indicates the region of close up in (B and C). (B–E) Two aggregates of β-gal+ cells appear in each hemisphere of the deep cerebellum in E16.5 *Math1*$^{LacZ/+}$ embryos (B). The medial aggregation is in the position of the fastigial deep cerebellar nucleus, and a close up (D) shows that most cells in this region are β-gal+. This β-gal expression is absent in *Math1*$^{LacZ/-}$ embryos (C and E). (Asterisks indicate rRL.) (F and G) Nissl (cresyl violet) staining in comparable regions at E18.5 shows a distinct nucleus (F) that appears to be gone in *LacZ*/– embryos (G), replaced by cells with different morphologies. (H and I) *Lhx9* mRNA is expressed in the same region (H) and is lost in *LacZ*/– embryos (I). (J–S) Tbr-1 is also expressed in the same region (J, M, and O) and is similarly lost in *LacZ*/– embryos (K, Q, and S). The large boxes indicate the regions shown in (L), (M), (P), and (Q), and the small boxes indicate the regions shown in (N), (O), (R), and (S). TOTO-3 nuclear colabeling in the *LacZ*/+ embryos shows cells with large nuclei that express Tbr-1 (arrows) and cells with small nuclei that do not (arrowheads) (N and O). In the *LacZ*/– embryos, the same region contains only cells with small nuclei that do not express Tbr-1 (arrowheads) (R and S). Abbreviations: EGL, external granule layer; L, lateral deep cerebellar nucleus; *Lhx9*, *LIM-homeodomain nine* antisense mRNA; M, medial deep cerebellar nucleus; Tbr-1, anti-T-box-related one protein. Scale bar, 250 μm (B and C); 85 μm (D–K); 40 μm (L, M, P, and Q); 18 μm (N, O, R, and S).

topic calbindin staining (data not shown), probably corresponding to ectopic Purkinje cells (Ben-Arie et al., 1997; Jensen et al., 2002). This study indicates that at least a subset of deep nuclear neurons of the cerebellum are derived from the rhombic lip and are *Math1* dependent.

The Cochlear Extramural Stream Generates the Ventral Cochlear Nucleus and Cochlear Granule Neurons and Is *Math1* Dependent

At E12.5, while the deep nuclear neurons of the cerebellum migrate from the rRL, another group of β-gal+ cells migrates from the *Math1* expression domain in the lateral medulla. This region is contiguous with the rRL, and we refer to it as the caudal RL (cRL) (Figure 6A). The region into which these cells migrate is the developing cochlear nucleus (CN). Hence, we term this migration the "cochlear extramural stream" (CES) of the cRL. Just like the RLS, the CES cells appear to migrate superficially over the surface of more medial cells. At E14.5, as the RLS gives rise to the EGL in the cerebellum, the CES continues to add cells to the CN, and at E18.5, when the EGL fully covers the cerebellum, a contiguous group of β-gal+ cells covers portions of the CN (Figure 6A) in the position of the cochlear granule neurons (Martin and Rickets, 1981). Thus, β-gal+ cells contribute to both the cerebellum and CN at similar times during development.

The CN is anatomically divided into dorsal (DC) and ventral (VC) portions (Figure 6B). From E12.5 to E18.5, the CES extends from the cRL along the ventrolateral surface of the developing DC (Figures 6C–6F). A close up of the cRL at E12.5 shows the tangentially oriented stream of β-gal+ cells (Figure 6K). Many of these cells form a distinct cluster ventrolateral to the DC, in the position of the developing VC (Figures 6L and 6M). At E16.5, the eighth cranial nerve can be seen entering the ventral edge of this cluster (Figure 6M). Several β-gal+ cells also migrate obliquely into the DC from E12.5 to E18.5 (Figures 6S–6V). Such oblique migration has been described for the DC fusiform (pyramidal) projection neurons (early) and granule neurons (late) (Ivanova and Yuasa, 1998). In addition, β-gal+ fibers project ventrally

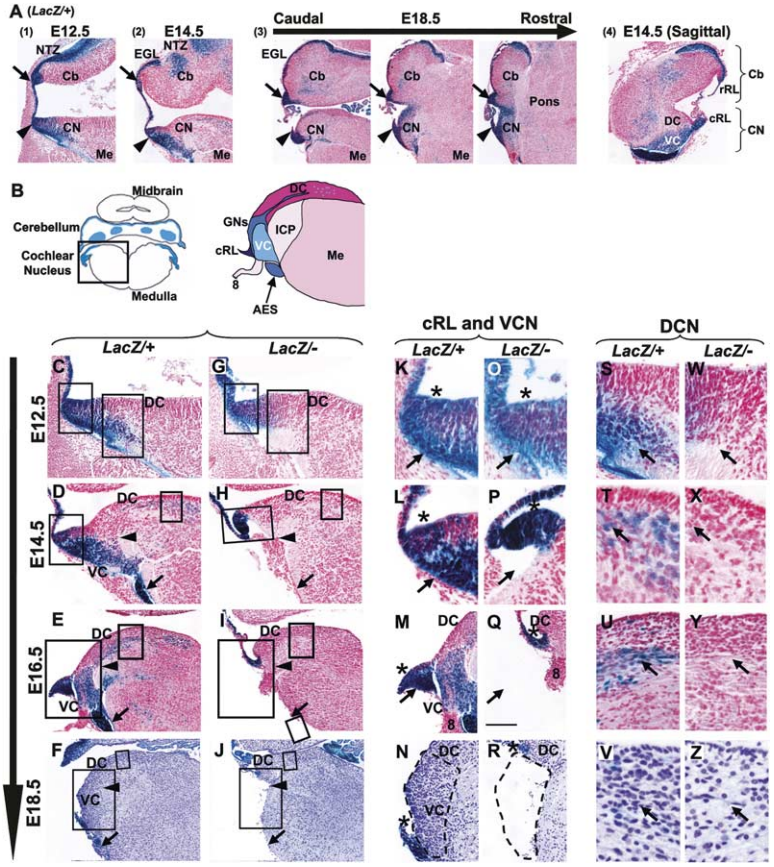

Figure 6. The Cochlear Extramural Stream of the Rhombic Lip Forms the Ventral Cochlear Nucleus and Cochlear Granule Neurons

All coronal sections are oriented with lateral to the left. (A) Parallel development of the cerebellum and CN. Coronal sections through *Math1*$^{LacZ/+}$ embryos at E12.5 (A1), E14.5 (A2), and E18.5 (A3) show β-gal expression extending at each time point from the rRL (arrow) and cRL (arrowhead) into the cerebellum and CN, respectively. At E18.5, the EGL and cochlear granular layer appear to merge laterally. (A4) A sagittal section at E14.5 shows that the medial neuroepithelia of the cerebellum and CN merge as well (caudal is to the right). (B) Two schematics are shown. The relative level of section and area of close up (box) shown in (C–J) are indicated at left. The substructure of the CN and neighboring region of medulla are depicted at right. (C–J) β-gal expression in the CN of *Math1*$^{LacZ/+}$ (C–E) and *Math1*$^{LacZ/-}$ (G–I) embryos at E12.5–E16.5. Nissl staining at E18.5 shows selective loss of the ventral portion of the CN in *LacZ*/– embryos (F and J). The DC/VC junction (arrowheads) and the AES (arrows) and their expected locations in the *LacZ*/– embryos are indicated. Lateral and medial boxes indicate regions of close up shown in (K)–(R) and (S)–(Z), respectively. (K–R) The CES, GNs, and entire VC are missing in *LacZ*/– embryos (O–R) compared to *LacZ*/+ embryos (K–N) (asterisks indicate ventricular surface of cRL; arrows indicate position of CES). Dotted line in (R) shows complete absence of VC. (S–Z) Select cells of the DC are also missing in *LacZ*/– embryos (W–Z) compared to *LacZ*/+ embryos (S–V) (arrows indicate expected positions of β-gal+ cells). Abbreviations: 8, cranial nerve eight; AES, anterior precerebellar extramural migratory stream; Cb, cerebellum; CN, cochlear nucleus; cRL, caudal rhombic lip; DC, dorsal cochlear nucleus; EGL, external granule layer; GNs, cochlear granule neurons; ICP, inferior cerebellar peduncle; Me, medulla; NTZ, nuclear transitory zone; rRL, rostral rhombic lip; VC, ventral cochlear nucleus. Scale bar, 350 μm (A3); 270 μm (A4); 220 μm (A1, A2, E, F, I, and J); 140 μm (M and Q); 125 μm (C, D, G, and H); 105 μm (N and R); 50 μm (K, L, O, and P); 60 μm (S, V, U, and Y); 35 μm (T, X, V, and Z).

from the CN at E12.5 (Figure 6S). In the absence of *Math1*, the CES does not form, the cRL appears shrunken, and the VC is lost (Figures 6O–6Q). In contrast, the bulk of the DC remains, although the β-gal+ staining in the deep DC is lost (Figures 6W–6Y). The eighth cranial nerve enters directly into this residual DC structure (Figure 6Q). Nissl staining at E18.5 confirms the complete loss of the VC in *Math1*$^{LacZ/-}$ embryos (Figure 6R) and indicates a decrease in cell density in the DC (Figure 6Z). These results demonstrate a previously unrecognized genetic division in the development of the CN and show that the granule neurons and VC derive from the cRL, whereas much of the DC arises from the more medial neuroepithelium.

The RL also gives rise to a diffuse population of β-gal+ cells in the superior vestibular nucleus (SuVe) (Figure S1D available with this article online), although it is not clear whether these cells originate in the rRL or cRL. The SuVe has been postulated to form adjacent to the NTZ (Altman and Bayer, 1985), and similar to the developing fastigial nucleus, some SuVe cells express Tbr-1 (R. Hevner, personal communication) (Figure S1H). In the absence of *Math1*, both β-gal and Tbr-1 expression is lost (Figures S1E and S1K). These results suggest that the vestibular nuclei consist of a mixture of cells derived from the rhombic lip and from more medial neuroepithelium.

All Mossy-Fiber Precerebellar Nuclei Require *Math1*

Four-brainstem nuclei are thought to derive from the cRL and project mossy fibers to the granule and deep nuclear neurons of the cerebellum. The reticulotegmental (Rtgn) and basal pontine gray (PN) nuclei migrate in the anterior precerebellar extramural migratory stream (AES) (Altman and Bayer, 1987d), whereas the lateral reticular (LRt) and external cuneate (ECN) nuclei migrate in the posterior precerebellar extramural migratory stream (PES) (Altman and Bayer, 1987c). Serial coronal sections at E14.5 show that β-gal expression is continuous in the cRL from the CN to the caudal medulla (Figures 7A and 7B). As expected, the portion of the cRL immediately caudal to the CN (Figures 7C and 7D) appears to generate a superficial stream of β-gal+ cells in the location of the AES (Figure 7E). Similarly, a superficial stream of β-gal+ cells in the region of the PES (Figure 7K) is contiguous with an even more caudal portion of the cRL (Figure 7I and 7J). By E18.5, the AES cells settle in the ventral pons, clearly forming the Rtgn and PN (Figure 7O), and the PES cells settle in the ventral medulla in the region of the LRt (Figure 7S). They

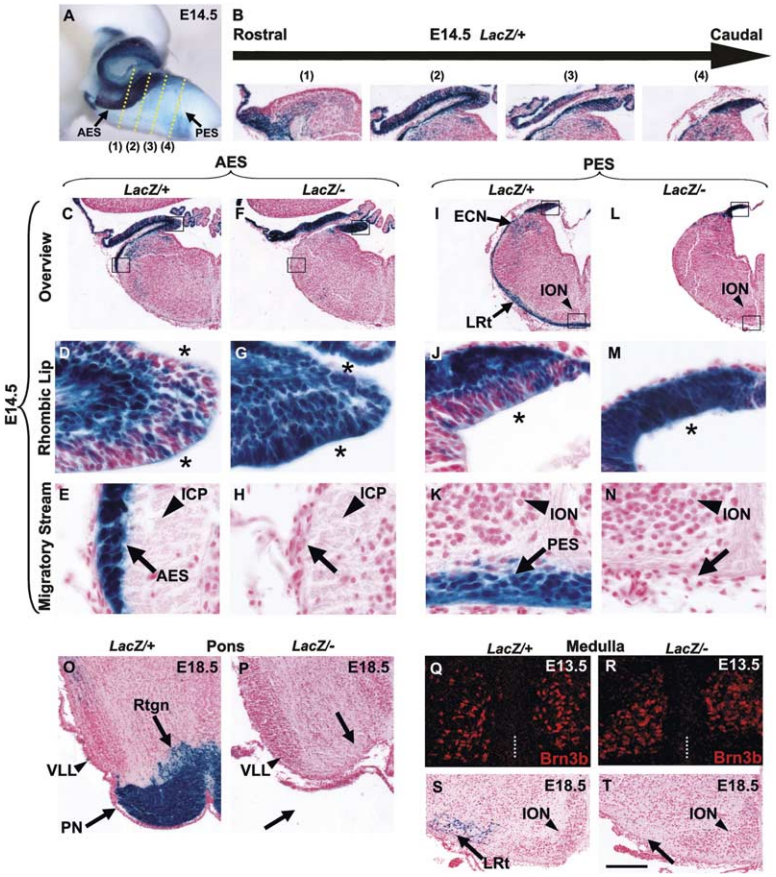

Figure 7. Mossy-Fiber Precerebellar Neurons Derive from *Math1*-Expressing Progenitors, But the Inferior Olive Does Not

All coronal sections are oriented with lateral to the left. (A and B) A whole-mount E14.5 *Math1*$^{LacZ/+}$ hindbrain (A) shows β-gal+ cells migrating from the cRL in the AES and PES to the ventral pons and medulla, respectively. Yellow lines indicate the levels of adjacent coronal sections through the medulla (B) showing the transition of the cRL from the cochlear nucleus to the caudal medulla. (The different appearances of the cRL are partially due to bends of the hindbrain toward and away from the section plane.) (C–H) At E14.5, the AES migrates from the cRL in *LacZ*/+ (C) but not in *LacZ*/– (F) embryos. Close ups show that although the cRL continues to express β-gal in *LacZ*/– embryos (compare [D] and [G]), the AES is completely lost, whereas the inferior cerebellar peduncle is still present (compare [E] and [H]). (Asterisks indicate ventricular surface of cRL.) (I–N) The PES migrates from a more caudal portion of the cRL in *LacZ*/+ (I) but not in *LacZ*/– (L) embryos. This portion of the cRL also continues to express β-gal in *LacZ*/– embryos (compare [J] and [M]), and the PES is similarly completely lost (compare [K] and [N]). In contrast, the ION neurons do not express β-gal (K) and are not lost in the *LacZ*/– embryos (N). (Asterisks indicate ventricular surface of cRL.) (O and P) At E18.5, the Rtgn and PN are both β-gal+ in the *LacZ*/+ embryos (O) and are lost in the *LacZ*/– embryos (P). In contrast, the VLL is present in both. (Q and R) The ION correctly expresses Brn3b at E13.5 in both *LacZ*/+ (Q) and *LacZ*/– (R) embryos. Dotted lines indicate the midline of the medulla. (S and T) At E18.5, the LRt is also β-gal+ in the *LacZ*/+ embryo (S), and this expression is similarly absent in the *LacZ*/– embryo (T). In contrast, the ION is still present (compare [S] and [T]). Abbreviations: AES, anterior precerebellar extramural migratory stream; Brn3b, anti-Brn3 POU-domain transcription factor b; ECN, external cuneate nucleus; LRt, lateral reticular nucleus; ICP, inferior cerebellar peduncle; ION, inferior olive nucleus; PES, posterior precerebellar extramural migratory stream; PN, pontine nucleus; Rtgn, reticulotegmental nucleus; VLL, ventral nucleus of the lateral lemniscus. Scale bar, 235 μm (B); 320 μm (C, F, I, and L); 35 μm (D, E, G, H, J, K, M, and N); 240 μm (O and P); 60 μm (Q and R); 200 μm (S and T).

also settle in the dorsal medulla in the region of the ECN (data not shown). Previous studies showed that the PN and ECN require *Math1* to form (Ben-Arie et al., 2000; Bermingham et al., 2001). We now show that in the absence of *Math1*, the cRL appears thinner, although it still expresses β-gal (Figures 7G and 7M), the AES and PES fail to form (Figures 7H and 7N), and all four mossy-fiber precerebellar nuclei are lost (Figures 7P and 7T).

In contrast, the cells of the inferior olive nucleus (ION) do not express β-gal at E14.5 and are clearly present in both *Math1*$^{LacZ/+}$ and *Math1*$^{LacZ/-}$ embryos at E14.5 (Figures 7K and 7N) and at E18.5 (Figures 7S and 7T). Furthermore, ION neurons normally express Brn3b (Pou4f2) at E13.5 (Marillat et al., 2004), and this expression is still present in the absence of *Math1* (Figures 7Q and 7R). It is noteworthy that the entire length of the cRL expresses β-gal throughout the time of ION formation (Figure 2B) and that although β-gal+ cells are generated during this time, they do not contribute to the ION. These data demonstrate that the inferior olive does not derive from *Math1*-expressing progenitors in the rhombic lip and strengthen the evidence that mossy fiber and inferior olive precerebellar neurons have separate genetic lineages.

Discussion

In this study, we use β-gal driven by the *Math1*^{lacZ} allele to trace the migration of rhombic-lip-derived cells in the hindbrains of *Math1*$^{lacZ/+}$ and *Math1*$^{lacZ/-}$ mice. Our analysis provides new insights into the origins of neurons in the deep cerebellar, cochlear, precerebellar, lateral lemniscal, and parabrachial nuclei. We demonstrate that cells derived from *Math1*-expressing progenitors share characteristics including the expression and requirement of *Math1*, origins in the rhombic lip, superficial migration during a portion of their transit, and contribution to the proprioceptive/vestibular/auditory sensory network. These observations reveal similarities in the development of the cerebellum and cochlear nucleus and lead us to propose a novel genetic definition for the rhombic lip.

The Rhombic Lip Generates Similar Neurons of the Cerebellum and Cochlear Nucleus

The cerebellum and cochlear nucleus (CN) contain some similar cell types and organization, such as distinct regions of granule, inhibitory, and projection neurons. Several of these neurons appear to function analogously in each structure, and the granule neurons of

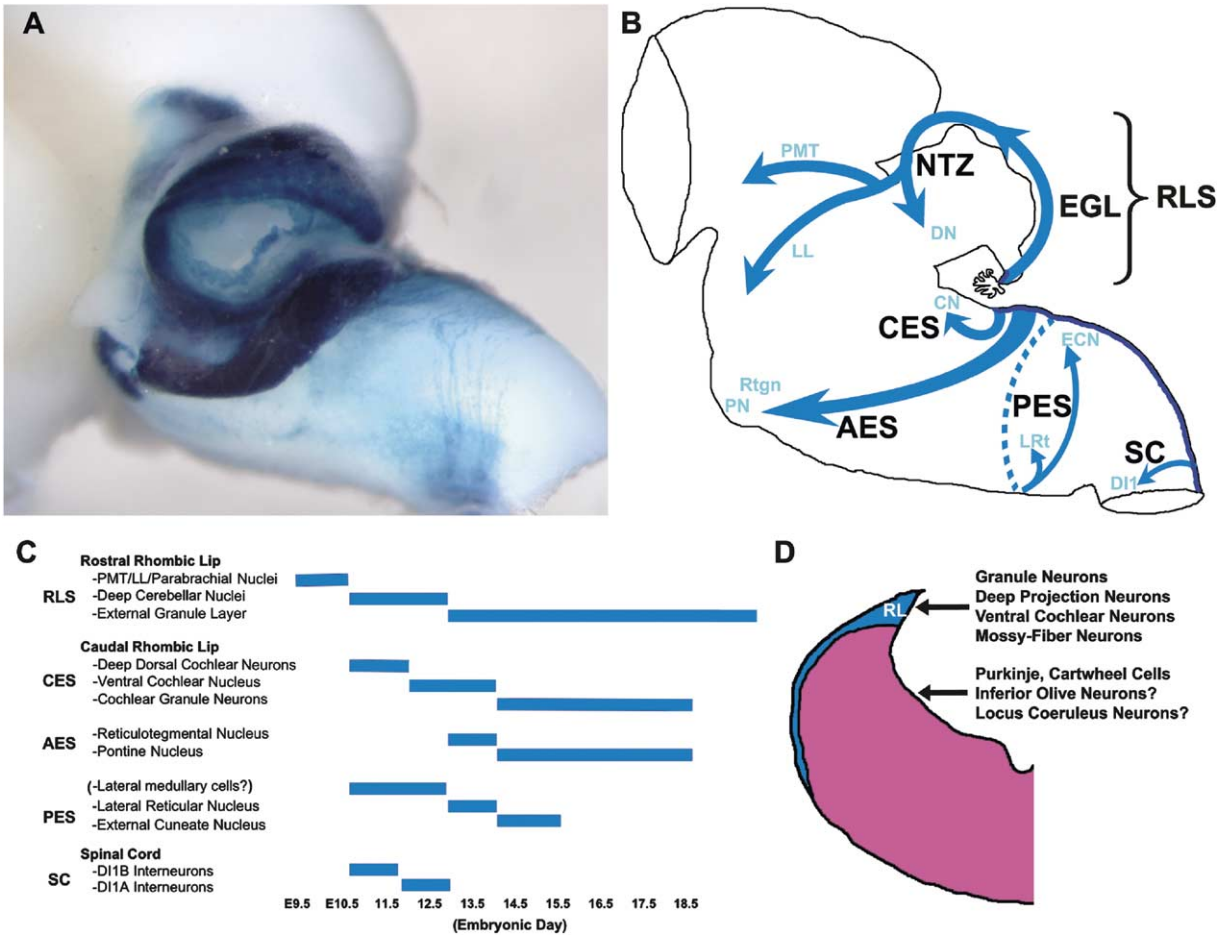

Figure 8. Summary Schematic of Migratory Streams from the Rhombic Lip

(A) A whole-mount E14.5 *Math1*$^{LacZ/+}$ hindbrain shows the β-gal-expressing migratory streams from the RL (rostral to left).

(B) Schematic of the hindbrain depicts each of these RL migratory streams and the locations in which their cells settle. The dotted line of the PES indicates that these cells migrate from one side of the medulla, cross the midline, and settle on the other side. SC is the β-gal+ stream that arises from the *Math1*-expressing dorsal spinal cord neuroepithelium, which is contiguous with the RL.

(C) Schematic showing the approximate migration time from the RL for each of the RL-derived cell types as well as from the contiguous region in the spinal cord.

(D) Schematic showing a coronal section through the hindbrain and indicating the proposed redefinition of the RL as the *Math1*-expression zone of the ventricular neuroepithelium of the rhombencephalon. Abbreviations: AES, anterior precerebellar extramural migratory stream; CES, cochlear extramural stream; CN, cochlear nucleus; DN, deep cerebellar nuclei; DI1, type one spinal cord dorsal interneurons; ECN, external cuneate nucleus; EGL, external granule layer; LL, lateral lemniscus; LRt, lateral reticular nucleus; NTZ, nuclear transitory zone; PES, posterior precerebellar extramural migratory stream; PMT, pontomesencephalic tegmentum; PN, pontine nucleus; RLS, rostral rhombic-lip migratory stream; Rtgn, reticulotegmental nucleus; SC, spinal cord.

each receive some parallel input from the mossy fiber precerebellar nuclei (Altman and Bayer, 1980; Ivanova and Yuasa, 1998; Oertel and Young, 2004). However, the developmental relationship between these cells has been uncertain. We show that some analogous cell types of the cerebellum and CN derive from the same dorsal-ventral region of the hindbrain neuroepithelium and require the same proneural transcription factor for their development.

Our data provide the first direct evidence that at least some deep nuclear neurons (DNs) of the cerebellum arise from the rostral rhombic lip (rRL) rather than from the more ventromedial ventricular neuroepithelium. This cell population is derived from the early portion of the rostral rhombic-lip migratory stream (RLS) that leaves the rRL beginning around E10 and is distinct from the later portion of the RLS that forms the EGL beginning around E13. We are convinced that these cells are DNs for the following reasons. First, the timing of this initial migration correlates well with the birthdates of the DNs, most of which are born between E10 and E12 (Taber-Pierce, 1975). Second, these cells aggregate superficially in the developing cerebellum in the region of the nuclear transitory zone (Altman and Bayer, 1985) and then descend ventrally. Third, they extend processes into the superior cerebellar peduncle (SCP) and the uncinate fasciculus, also characteristic of DNs. Their transient superficial aggregation in the position of the developing SCP may facilitate their projection through this fiber tract. Finally, in the absence of *Math1*, the loss of the RLS correlates with loss of *Lhx9* and *Tbr-1* expression and with the disappearance of large neurons from

the expected regions of the deep cerebellar nuclei. These data demonstrate that the EGL is the last portion of a superficial rostral rhombic-lip migratory stream that begins much earlier and that also forms deep nuclear neurons of the cerebellum.

Previous studies suggested that deep nuclear neurons and granule neurons of the cerebellum have distinct neuroepithelial origins (Hatten and Heintz, 1995). Quail-chick transplantation studies suggested that many cerebellar cell types, including the DNs and PCs, derive from both the midbrain and hindbrain, whereas the granule neurons derive primarily from the hindbrain (Hallonet et al., 1990). However, more recent studies have shown that the anatomic constriction used for these transplant studies does not correlate with the midbrain-hindbrain boundary and that all these cerebellar cell types actually derive entirely from the hindbrain (Millet et al., 1996). We now demonstrate that a large number of DNs derive from the rRL of the hindbrain. Thus, it is possible that a portion of the rRL was inadvertently transplanted in those previous studies. It is also possible that distinct subsets of DNs arise from both the rRL and from more medial portions of the neuroepithelium. Additional DN markers may help clarify this possibility. Studies using clonal analysis with LacZ mosaics and retroviral injections rarely find animals in which DNs and granule neurons are both labeled (Lin et al., 2001; Mathis et al., 1997). Thus, although some DNs share *Math1* dependence with the granule neurons and migrate from the same region, they may still derive from different progenitors within the rRL.

We also find that the ventricular neuroepithelium of the developing cochlear nucleus contains a lateral *Math1*-expression domain that is contiguous with the rRL and a medial non-*Math1*-expression domain that is contiguous with the cerebellar neuroepithelium that generates the Purkinje cells. The dorsal subdivision (DC) of the CN contains distinct layers of granule neurons, inhibitory cartwheel cells, and deep projection neurons, similar to the cerebellum, and functions to discriminate between sounds (Oertel and Young, 2004). The ventral subdivision (VC) forms a compact nucleus ventrolateral to the DC and contains several types of projection neurons involved in sensing the organism's position with respect to a sound (Cant and Benson, 2003). Our data reveal that the VC shares a neuroepithelial origin with the cochlear granule neurons rather than with the bulk of the DC. The VC is derived from an early portion of the cochlear extramural stream (CES) of the caudal RL (cRL) beginning around E12, whereas the cochlear granule neurons arise from a later portion of the CES. We propose that the CES forms the VC for the following reasons. First, the timing of migration correlates well with the birthdates of the VC neurons, most of which are formed from E12–E13 (Martin and Rickets, 1981; Taber-Pierce, 1967). Second, the cells aggregate in the known region of the developing VC. Third, in the absence of *Math1*, the loss of the CES correlates with the loss of the VC. Similarly, the timing of migration of late cRL-derived cells correlates with the formation of the cochlear granule neurons from E14.5 through birth (Martin and Rickets, 1981). These cells settle in the expected granule cell domain of the CN, and just like the VC, this layer is lost in the absence of *Math1*.

These data suggest that a shared developmental pathway that is dependent on *Math1* operates in both the cerebellum and cochlear nucleus. RL-derived cells simultaneously populate both structures, migrate superficially for part of their transit, require *Math1*, and give rise to analogous cell types (Figures 8A–8C). Early-migrating cells appear to form large projection neurons, whereas later-migrating cells form granule neurons. Similarly, the contiguous ventromedial neuroepithelium forms non-*Math1*-dependent neurons of each structure. Our results reveal novel genetic divisions within the cerebellum and cochlear nucleus and may help explain the similar cell types of these adjacent hindbrain processing centers.

A Proposal for a Refined Definition of the Rhombic Lip

Many boundaries exist between different cell populations in the developing embryo. Some of these boundaries are approximated by gross anatomical characteristics, such as flexures of the neural tube that were used for many years to define the boundaries of the developing cerebellum (Hallonet et al., 1990; Hatten and Heintz, 1995). However, more recent studies show that these cerebellar boundaries are much more accurately delineated by the molecular expression patterns of *Otx2* and *Hoxa2* (Millet et al., 1996; Wingate and Hatten, 1999). The rhombic lip has long been recognized as a distinct structure that produces functionally related neuronal populations, but its dorsal-ventral extent has remained loosely defined by an anatomical bend in the ventricular neuroepithelium that appears near the onset of EGL formation, around E13 (Altman and Bayer, 1997; Wingate, 2001). Prior to that time, there has been no method to distinguish the rhombic lip from the more ventromedial neuroepithelium.

We show that *Math1* expression identifies the region in the ventricular neuroepithelium that delimits the origins of hindbrain neurons that undergo superficial migration (Figure 8D). Importantly, these *Math1*-dependent cells include most of the populations classically thought to derive from the RL, such as the cerebellar and cochlear granule neurons and all the mossy-fiber precerebellar nuclei, and exclude populations thought to derive from more medial regions, such as the Purkinje cells. Yet, the loose anatomical definition of the RL has caused some cell populations with very different characteristics, such as the inferior olive nucleus (ION) and locus coeruleus (LC) neurons, to be grouped with these *Math1*-dependent cells (Essick, 1912; Harkmark, 1954; Lin et al., 2001).

Some previous morphological studies suggest that the ION forms from more ventromedial portions of the neuroepithelium rather than from the RL (Altman and Bayer, 1987b; Ellenberger et al., 1969), and recent studies indicate that the ION neurons have a different genetic lineage from the mossy-fiber neurons (Funfschilling and Reichardt, 2002; Li et al., 2004; Rodriguez and Dymecki, 2000). These distinguishing characteristics of the ION raise the possibility that it derives from a different region of the ventricular neuroepithelium

than the mossy-fiber precerebellar nuclei. Ablation studies demonstrate that to completely eliminate the ION, the entire dorsal third of the ventricular neuroepithelium must be removed (de Diego et al., 2002; Harkmark, 1954). In addition, the ION intramural migratory stream appears to form ventromedial to the origin of the superficial streams (de Diego et al., 2002). This observation is supported by studies of human ION dysplasias in which ION neurons prematurely arrest in their migration and settle near the medial neuroepithelium, suggesting that at least some ION neurons arise from this medial region of the neuroepithelium rather than from the RL (Friede, 1989). Our results demonstrate that the ION neurons do not derive from *Math1*-expressing progenitors and confirm that these neurons do not require *Math1* to form an anatomically intact ION. Like the neurons of the ION, the LC noradrenergic neurons are not *Math1* dependent, as demonstrated by the continued presence of tyrosine hydroxylase expression (Figure S2). Rather, these LC neurons require a different proneural gene, *Mash1*, as do the other noradrenergic neurons in both the hindbrain and peripheral nervous system (Hirsch et al., 1998). Similar to the Purkinje cells, the LC and ION may arise from more medial portions of the ventricular neuroepithelium. Indeed, a recent study shows that the bHLH gene *Ptf1a* is expressed in this medial region and not in the RL, and labels Purkinje cells and ION neurons (Hoshino et al., 2005).

At all rostral-caudal levels along the rhombencephalon, cells derived from *Math1*-expressing progenitors stretch from the ventricular to the superficial surface in an initial short radial migration followed by a switch to tangential orientation to form the superficial migratory streams of the hindbrain. As a result, the RL usually appears composed of two layers. In the absence of *Math1*, this two-layered structure collapses into a single-layered cluster of cells, and the migratory streams are lost. Based on our observations, we propose that the rhombic lip should be thought of as a functionally distinct portion of the hindbrain neuroepithelium that generates superficial migratory streams and that its cells can be genetically identified by *Math1* expression.

Math1 Is Required for Central and Peripheral Components of the Proprioceptive/Vestibular/Auditory Sensory Network

An outstanding question in neurodevelopment is how various neurons arising in different portions of the neural tube are organized into functional systems. Three such systems, the proprioceptive, vestibular, and auditory systems, work together to sense the organism's position in space. Previous studies show that some of the hindbrain neurons involved in these systems are *Math1* dependent: the cerebellar granule neurons and some mossy-fiber precerebellar nuclei (Ben-Arie et al., 1997, 2000; Bermingham et al., 2001). We now demonstrate that *Math1* is required for many additional components of these same systems, including deep neurons in the cerebellum and dorsal cochlear nucleus, the entire ventral cochlear nucleus and cochlear granule neurons, a subset of cells in the vestibular nuclei, the remainder of the mossy-fiber precerebellar nuclei, and neurons in the parabrachial nuclei (PB) and along the auditory tracts in the lateral lemnisci (Figures 8A–8C). In addition, some cell populations derived from *Math1*-expressing progenitors are not readily identifiable with available markers, and some take migration paths that we are not able to follow in the current study. These cells will require further characterization to determine if they also participate in these systems.

The role of the PB in these systems has only recently been uncovered. The PB surrounds the superior cerebellar peduncle, the output track for the deep cerebellar nuclei, and is theorized to arise from the rostral NTZ, adjacent to the developing deep nuclear neurons of the cerebellum (Altman and Bayer, 1985). Our results demonstrate that at least some PB neurons derive from the RLS just like the DNs. A few recent reports in chicken and fish describe unidentified cells that appear to migrate from the rRL to the pons and isthmus (Koster and Fraser, 2001; Lin et al., 2001; Wingate and Hatten, 1999) and may represent similar cells of the RLS in those species. The PB appears to regulate aspects of respiratory, cardiac, and intestinal function (Balaban et al., 2002). Subsets of the PB neurons are connected with the vestibular nuclei and are activated in response to various body movements. Activation of the vestibular system has long been known to affect breathing, blood pressure, and intestinal activity, such as the nausea often associated with spinning. Recent studies suggest that the PB mediates these responses by integrating proprioceptive/vestibular sensory information with sensation from inner organs (Balaban et al., 2002). Thus, as with all the other rhombic-lip-derived neurons, the *Math1*-dependent parabrachial neurons participate in the proprioceptive/vestibular/auditory sensory network.

The rhombic lip is contiguous caudally with the *Math1*-expressing region in the dorsal spinal cord (Figure 8B). This region generates the dI1 interneurons of the proprioceptive system (Figure 8C), which relay input from peripheral mechanoreceptors, such as the cutaneous Merkel cells, to the cerebellum. Like the RL-derived precerebellar neurons, these spinal cord neurons require *Math1* and project to the cerebellar granule neurons via mossy fibers (Bermingham et al., 2001). In addition, several peripheral mechanoreceptors, including the Merkel cells and the auditory and vestibular inner ear hair cells, are likewise *Math1* dependent (Ben-Arie et al., 2000; Bermingham et al., 1999). The requirement of *Math1* in at least the peripheral components of these systems is well conserved since the fly homolog of *Math1*, *atonal*, is similarly required for the proprioceptive and auditory peripheral mechanoreceptors in flies (Jarman et al., 1993). Thus, these various neurons express and require the same proneural gene and connect with each other to form large portions of the proprioceptive/vestibular/auditory sensory network.

In summary, we identify several novel populations of rhombic-lip-derived neurons and demonstrate novel genetic divisions in the formation of the cerebellum and cochlear nucleus. Based on these observations, we propose a refined definition of the rhombic lip as consisting of the *Math1*-expressing neuroepithelium along the fourth ventricle. This genetic definition may help clarify the lineage relationships between neurons involved in certain developmental disorders of the hindbrain. An important next step will be to identify the

genes that determine the fates of *Math1*-expressing cells arising at different times and from different anterior-posterior portions of the rhombic lip. Interestingly, the *Math1*-dependent central neurons arise from the same relative dorsal-ventral position of the neural tube and contribute to the same sensory network. It is possible that other systems may be similarly integrated throughout the spinal cord, hindbrain, and peripheral nervous system by their expression and dependence on specific transcription factors. Better understanding of the developmental origins and genetic lineages of cells within specific neuronal networks may give us insights into the connectivity, function, and evolution of these systems.

Experimental Procedures

Mouse Strains, Staging, and Genotyping

This study used two null alleles of *Math1* that contain either *LacZ* (*Math1*^{LacZ}) or *HPRT* (*Math1*$^{-}$) in place of the *Math1* open-reading frame (Ben-Arie et al., 1997, 2000). The null embryos carried one *Math1*^{lacZ} allele and one *Math1*$^{-}$ allele to ensure equal dosing of *LacZ* when comparing to *Math1*$^{lacZ/+}$ embryos. For staging, noon on the day that the vaginal plug was observed was counted as embryonic day 0.5 (E0.5). Yolk sacs or tails were collected before fixation for PCR genotyping: *Math1*-3′ reverse primer (5′-GGCACT GGCTTCTCTTGG-3′), *Math1*-3′ forward primer (5′-ACGCACTTC ATCACTGGC-3′), Neo 3′ forward primer (5′-GCATCGCCTTCTAT CGCC-3′), for a wt band of 600 bp and a LacZ null band of 350 bp. Genotypes of embryos used in the final analysis were verified by Southern as previously described (Ben-Arie et al., 1997). All animals were housed in a pathogen-free mouse colony in compliance with the guidelines of the Center of Comparative Medicine of Baylor College of Medicine.

X-Gal Staining, Immunohistochemistry, and RNA In Situ Hybridization

Embryos were collected at E10.5, E11.5, E12.5, E13.5, E14.5, E15.5, E16.5, and E18.5. Embryos were examined as whole mounts and by serial sectioning. For each time point, approximately ten *Math1*$^{lacZ/+}$ and ten *Math1*$^{lacZ/-}$ embryos were examined with serial sections through the entire hindbrain in coronal, sagittal, and transverse planes for a total of 160 embryos. Images from 42 of these embryos are shown.

β-galactosidase (β-gal) activity was assayed by staining tissues with X-gal (1 mg/ml) followed by paraffin imbedding, as previously described (Ben-Arie et al., 2000). The brain was isolated from E14.5 and older embryos, whereas the whole embryo was stained for younger ages. 5-μm paraffin sections were counterstained with nuclear fast red or with cresyl violet for Nissl staining (Bermingham et al., 2001).

For immunolabeling, 5-μm paraffin sections and 12-μm frozen sections were cut. For paraffin sections, heat antigen retrieval with 0.01 M citrate buffer (pH 6.0) was performed. Primary and secondary antibody staining was performed as previously described (Bermingham et al., 2001). The source and final dilution of antibodies is available as in the Supplemental Experimental Procedures.

In situ hybridization was performed with DIG-labeled antisense RNA probes to *LacZ* and *Lhx9.* Frozen sections were postfixed with 4% paraformaldehyde and briefly treated with 3 μg/ml proteinase K. Hybridization was performed at 65°C overnight in hybridization buffer (50% formamide, 5× SSC [pH 4.5–5.0], 1% SDS, 50 μg/ml yeast tRNA, 50 μg/ml heparin) after 2 hr of prehybridization. Slides were washed three times with washing buffer (50% formamide, 1× SSC [pH 4.5–5.0], 1% SDS) and then incubated with phosphatase-conjugated anti-DIG antibody (1:500, Roche) in MABT (100 mM maleic acid, 150 mM NaCl, 0.1% Tween 20 [pH 7.5]), 2% Blocking Reagent (Roche), and 10% sheep serum overnight at 4°C. Slides were then washed five times with MABT plus 1% levamisole (Vector Labs) and once with NTMT (100 mM Tris-HCl [pH 9.5], 100 mM NaCl, 50 mM $MgCl_2$, 0.1% Tween 20, and 1% levamisole). BM Purple (Roche) was used to detect signals.

Fluorescent staining was examined by confocal microscopy (Zeiss Axiovert LSM 510 system). Nonfluorescent specimens were examined on a Zeiss Axioplan light microscope, and images were collected with a Zeiss AxioCam.

Neuroanatomical Correlation

Anatomical structures were determined by crossreferencing seven atlases (Altman and Bayer, 1995; Franklin and Paxinos, 1997; Jacobowitz and Abbott, 1997; Kaufman, 1992; Paxinos et al., 1994, 1999; Schambra et al., 1992) and one textbook (Altman and Bayer, 1997). In this study, all sagittal sections are oriented with caudal to the right. Thus, the RL is always located to the right in sagittal sections. Because coronal sections are symmetrical, only the left half of each is shown. Thus, all coronal half sections are oriented with lateral to the left. As a result, the RL is always located to the left in coronal sections.

Supplemental Data

The Supplemental Data for this article can be found online at http://www.neuron.org/cgi/content/full/48/1/31/DC1/.

Acknowledgments

We thank Dr. Robert Hevner (University of Washington, Seattle) for the Tbr-1 antibody and for sharing unpublished results and Bobby Antalffy (Baylor College of Medicine, Houston) for technical assistance with histological preparations. We also thank S. Maricich, D. Armstrong, A. Flora, G. Miesegaes, and N. Shroyer (Baylor College of Medicine) for comments on the manuscript. This work was supported by National Research Service Award Kirschstein Predoctoral Fellowships (M.F.R. and V.Y.W.), a Baylor Research Advocates for Student Scientists Scholarship (M.F.R.), a McNair scholarship (V.Y.W.), and the neuropathology core of the Baylor College of Medicine Mental Retardation Developmental Disabilities Research Center. H.Y.Z. is an Investigator of the Howard Hughes Medical Institute.

Received: May 31, 2005
Revised: July 5, 2005
Accepted: August 19, 2005
Published: October 5, 2005

References

Akazawa, C., Ishibashi, M., Shimizu, C., Nakanishi, S., and Kageyama, R. (1995). A mammalian helix-loop-helix factor structurally related to the product of *Drosophila* proneural gene atonal is a positive transcriptional regulator expressed in the developing nervous system. J. Biol. Chem. *270*, 8730–8738.

Altman, J., and Bayer, S.A. (1980). Development of the brain stem in the rat. I. Thymidine-radiographic study of the time of origin of neurons of the lower medulla. J. Comp. Neurol. *194*, 1–35.

Altman, J., and Bayer, S.A. (1985). Embryonic development of the rat cerebellum. I. Delineation of the cerebellar primordium and early cell movements. J. Comp. Neurol. *231*, 1–26.

Altman, J., and Bayer, S.A. (1987a). Development of the precerebellar nuclei in the rat: I. The precerebellar neuroepithelium of the rhombencephalon. J. Comp. Neurol. *257*, 477–489.

Altman, J., and Bayer, S.A. (1987b). Development of the precerebellar nuclei in the rat: II. The intramural olivary migratory stream and the neurogenetic organization of the inferior olive. J. Comp. Neurol. *257*, 490–512.

Altman, J., and Bayer, S.A. (1987c). Development of the precerebellar nuclei in the rat: III. The posterior precerebellar extramural migratory stream and the lateral reticular and external cuneate nuclei. J. Comp. Neurol. *257*, 513–528.

Altman, J., and Bayer, S.A. (1987d). Development of the precerebellar nuclei in the rat: IV. The anterior precerebellar extramural migratory stream and the nucleus reticularis tegmenti pontis and the basal pontine gray. J. Comp. Neurol. *257*, 529–552.

Altman, J., and Bayer, S.A. (1995). Atlas of Prenatal Rat Brain Development (Boca Raton, FL: CRC Press).

Altman, J., and Bayer, S.A. (1997). Development of the Cerebellar System: In Relation to its Evolution, Structure, and Functions (Boca Raton, FL: CRC Press).

Balaban, C.D., McGee, D.M., Zhou, J., and Scudder, C.A. (2002). Responses of primate caudal parabrachial nucleus and Kolliker-fuse nucleus neurons to whole body rotation. J. Neurophysiol. *88*, 3175–3193.

Ben-Arie, N., Bellen, H.J., Armstrong, D.L., McCall, A.E., Gordadze, P.R., Guo, Q., Matzuk, M.M., and Zoghbi, H.Y. (1997). Math1 is essential for genesis of cerebellar granule neurons. Nature *390*, 169–172.

Ben-Arie, N., Hassan, B.A., Bermingham, N.A., Malicki, D.M., Armstrong, D., Matzuk, M., Bellen, H.J., and Zoghbi, H.Y. (2000). Functional conservation of atonal and Math1 in the CNS and PNS. Development *127*, 1039–1048.

Bermingham, N.A., Hassan, B.A., Price, S.D., Vollrath, M.A., Ben-Arie, N., Eatock, R.A., Bellen, H.J., Lysakowski, A., and Zoghbi, H.Y. (1999). Math1: an essential gene for the generation of inner ear hair cells. Science *284*, 1837–1841.

Bermingham, N.A., Hassan, B.A., Wang, V.Y., Fernandez, M., Banfi, S., Bellen, H.J., Fritzsch, B., and Zoghbi, H.Y. (2001). Proprioceptor pathway development is dependent on Math1. Neuron *30*, 411–422.

Cant, N.B., and Benson, C.G. (2003). Parallel auditory pathways: projection patterns of the different neuronal populations in the dorsal and ventral cochlear nuclei. Brain Res. Bull. *60*, 457–474.

de Diego, I., Kyriakopoulou, K., Karagogeos, D., and Wassef, M. (2002). Multiple influences on the migration of precerebellar neurons in the caudal medulla. Development *129*, 297–306.

Ellenberger, C., Jr., Hanaway, J., and Netsky, M.G. (1969). Embryogenesis of the inferior olivary nucleus in the rat: a radioautographic study and a re-evaluation of the rhombic lip. J. Comp. Neurol. *137*, 71–79.

Essick, C.R. (1912). The development of the nuclei pontis and the nucleus arcuatus in man. Am. J. Anat. *13*, 25–54.

Franklin, K.B.J., and Paxinos, G. (1997). The Mouse Brain in Stereotaxic Coordinates (San Diego, CA: Academic Press).

Friauf, E. (1994). Distribution of calcium-binding protein calbindin-D28k in the auditory system of adult and developing rats. J. Comp. Neurol. *349*, 193–211.

Friede, R.L. (1989). Developmental Neuropathology, Second Revision and Expanded Edition (New York, NY: Springer-Verlag).

Funfschilling, U., and Reichardt, L.F. (2002). Cre-mediated recombination in rhombic lip derivatives. Genesis *33*, 160–169.

Hallonet, M.E., Teillet, M.A., and Le Douarin, N.M. (1990). A new approach to the development of the cerebellum provided by the quail-chick marker system. Development *108*, 19–31.

Harkmark, W. (1954). Cell migrations from the rhombic lip to the inferior olive, the nucleus raphe and the pons. A morphological and experimental investigation of chick embryos. J. Comp. Neurol. *100*, 115–209.

Hatten, M.E., and Heintz, N. (1995). Mechanisms of neural patterning and specification in the developing cerebellum. Annu. Rev. Neurosci. *18*, 385–408.

Hirsch, M.R., Tiveron, M.C., Guillemot, F., Brunet, J.F., and Goridis, C. (1998). Control of noradrenergic differentiation and Phox2a expression by MASH1 in the central and peripheral nervous system. Development *125*, 599–608.

His, W. (1891). Die Entwicklung des menschlichen Rautenhirns vom Ende des ersten bis zum Beginn des dritten Monats. I. Verlangertes Mark. Abhandlungen der koniglicher sachsischen Gesellschaft der Wissenschaften. Mathematische-physikalische Klasse *29*, 1–74.

Hoshino, M., Nakamura, S., Mori, K., Kawauchi, T., Terao, M., Nishimura, Y.V., Fukuda, A., Fuse, T., Matsuo, N., Sone, M., et al. (2005). Ptf1a, a bHLH transcriptional gene, defines GABAergic neuronal fates in cerebellum. Neuron *47*, 201–213.

Ivanova, A., and Yuasa, S. (1998). Neuronal migration and differentiation in the development of the mouse dorsal cochlear nucleus. Dev. Neurosci. *20*, 495–511.

Jacobowitz, D.M., and Abbott, L.C. (1997). Chemoarchitectonic Atlas of the Developing Mouse Brain (Boca Raton, FL: CRC Press).

Jarman, A.P., Grau, Y., Jan, L.Y., and Jan, Y.N. (1993). *atonal* is a proneural gene that directs chordotonal organ formation in the *Drosophila* peripheral nervous system. Cell *73*, 1307–1321.

Jensen, P., Zoghbi, H.Y., and Goldowitz, D. (2002). Dissection of the cellular and molecular events that position cerebellar Purkinje cells: a study of the math1 null-mutant mouse. J. Neurosci. *22*, 8110–8116.

Kaufman, M.W. (1992). The Atlas of Mouse Development (London: Academic Press).

Koster, R.W., and Fraser, S.E. (2001). Direct imaging of in vivo neuronal migration in the developing cerebellum. Curr. Biol. *11*, 1858–1863.

Li, S., Qiu, F., Xu, A., Price, S.M., and Xiang, M. (2004). Barhl1 regulates migration and survival of cerebellar granule cells by controlling expression of the neurotrophin-3 gene. J. Neurosci. *24*, 3104–3114.

Lin, J.C., Cai, L., and Cepko, C.L. (2001). The external granule layer of the developing chick cerebellum generates granule cells and cells of the isthmus and rostral hindbrain. J. Neurosci. *21*, 159–168.

Marillat, V., Sabatier, C., Failli, V., Matsunaga, E., Sotelo, C., Tessier-Lavigne, M., and Chedotal, A. (2004). The slit receptor Rig-1/Robo3 controls midline crossing by hindbrain precerebellar neurons and axons. Neuron *43*, 69–79.

Martin, M.R., and Rickets, C. (1981). Histogenesis of the cochlear nucleus of the mouse. J. Comp. Neurol. *197*, 169–184.

Mathis, L., Bonnerot, C., Puelles, L., and Nicolas, J.F. (1997). Retrospective clonal analysis of the cerebellum using genetic laacZ/lacZ mouse mosaics. Development *124*, 4089–4104.

Millet, S., Bloch-Gallego, E., Simeone, A., and Alvarado-Mallart, R.M. (1996). The caudal limit of Otx2 gene expression as a marker of the midbrain/hindbrain boundary: a study using in situ hybridisation and chick/quail homotopic grafts. Development *122*, 3785–3797.

Oertel, D., and Young, E.D. (2004). What's a cerebellar circuit doing in the auditory system? Trends Neurosci. *27*, 104–110.

Paxinos, G., Ashwell, K.W.S., and Tork, I. (1994). Atlas of the Developing Rat Nervous System, Second Edition (San Diego, CA: Academic Press).

Paxinos, G., Carrive, P., Wang, H., and Wang, P. (1999). Chemoarchitectonic Atlas of the Rat Brainstem (San Diego, CA: Academic Press).

Rodriguez, C.I., and Dymecki, S.M. (2000). Origin of the precerebellar system. Neuron *27*, 475–486.

Schambra, U.B., Lauder, J.M., and Silver, J. (1992). Atlas of the Prenatal Mouse Brain (San Diego, CA: Academic Press).

Taber-Pierce, E. (1966). Histogenesis of the nuclei griseum pontis, corporis pontobulbaris and reticularis tegmenti pontis (Bechterew) in the mouse. An autoradiographic study. J. Comp. Neurol. *126*, 219–254.

Taber-Pierce, E. (1967). Histogenesis of the dorsal and ventral cochlear nuclei in the mouse. An autoradiographic study. J. Comp. Neurol. *131*, 27–54.

Taber-Pierce, E. (1975). Histogenesis of the deep cerebellar nuclei in the mouse: an autoradiographic study. Brain Res. *95*, 503–518.

Wingate, R.J. (2001). The rhombic lip and early cerebellar development. Curr. Opin. Neurobiol. *11*, 82–88.

Wingate, R.J., and Hatten, M.E. (1999). The role of the rhombic lip in avian cerebellum development. Development *126*, 4395–4404.

Zhou, Q., and Anderson, D.J. (2002). The bHLH transcription factors OLIG2 and OLIG1 couple neuronal and glial subtype specification. Cell *109*, 61–73.